EFFECT OF CHANGES IN ENGINEERING DESIGN ON THE DISTRIBUTION OF REACTION PRODUCTS AND THE ELECTROCHEMICAL PROPERTIES OF TUBULAR ELECTRODES

ALFONS S. M. LINDHOLM

Department of Chemical Technology, Royal Institute of Technology, S-100 44 Stockholm (Sweden)

(Received March 26, 1982; in revised form August 26, 1982)

Summary

A characterization of two kinds of tubular electrodes has been made. A conventional double-wall tube was compared with a new type of single-wall tube.

The electrochemical behaviour of the latter was in all respects superior to the double-wall tubes. The overpotential at −18 °C as a function of the fill density was 10 - 20 mV lower for the single wall tube in the region 3.20 - 3.80 g/cm^3 and the differences increase strongly with increasing fill density. The differences in current distribution profiles are quite distinctive for the two types of electrodes. The progression of the reaction products through the active material was more uniform for the single wall tube electrode and, hence, resulted in an improved current efficiency. The easy mass transport through the tube wall and inside the pore system and the local effect of the reaction products had a great influence on the formation of the effective lead sulphate distribution.

Introduction

This study intends to show the influence of some important parameters on the function of the tubular lead dioxide electrode.

Because of the superior properties of tubular electrodes, a great number of batteries in the world designed for traction and stationary purposes use such positive plates. Their outer envelope is usually of cylindrical shape, and is nowadays made of different acid-resistant materials. The tube construction plays an important role in the capacity and service life of the battery.

With that in mind the construction must provide: high permeability for electrolyte and gas, low electrical resistance, good resistance against oxidation attack at temperatures up to 60 - 70 °C, high tensile strength, low deformability, sufficient bursting strength against internal pressure, and resistance to external abrasion.

0378-7753/83/$3.00

Being the container of the active material, the wall structure of the tubes is considered to be of prime importance. The fibres which constitute the tubes may be braided, woven or felted. The macrostructure defined by the mesh size for braided and woven tubes, and the density per square centimeter of the fibres for felted tubes, as well as the impregnating agent, determine the access of electrolyte to the pore system of the active material. The mechanical strength and deformability during operation as well as the apparent density of the active material determine, to a high degree, the electronic conductivity of the bulk material.

In addition, anomalous distributions of the discharge product, the cell geometry, and the polarization resistance are important factors which govern the discharge efficiency of the porous electrode.

Extensive work [1 - 14] regarding kinetic studies and developed discharge and potential profiles inside porous electrodes has been published in recent years. Contributions [15 - 18] on the morphological changes in the active material have shown new aspects of the discharge mechanism. The distribution of lead sulphate in flat plates, using the autoradiographic technique [19] and X-ray microprobe [20, 21], have manifested the formation and variation of sulphate barriers throughout the active material.

Tubes with good performance qualities have been used by several battery manufacturers for many years [22]. The demand for new and still better tubes has, however, increased in recent times. As a consequence, this study describes the characteristic properties of well established tube constructions as well as of tubes which are new products and the result of extensive experimental work. The influence of well modified physical tube construction, proper electrode geometry, and a balanced amount of active material is shown to be of the highest importance for the proper and regular distribution of reaction products throughout the electrode during its operation. The variations in internal resistance and polarization properties under different conditions are also discussed.

Experimental

Comparative electrical and electrochemical measurements have been carried out on tubular electrodes of different parameters. The two prime subjects were: the double wall tube, Tudor Pg (Fig. 1), with an inner sleeving of braided glass fibres surrounded by a perforated PVC wrapping, and the single wall tube, Tudor PgS (Fig. 2), made of braided glass fibres reinforced with axial warps. The length of all the tubes in the experimental cells was 135 mm and the inner diameter 8.4 mm. The effective length was 126 mm and, consequently, the effective volume was 5.83 cm^3 and the geometrical area 33.25 cm^2. For determination of the current distribution the spine diameter was 3.0 mm in all cells and the tube diameter 8.4 mm. In some electrochemical tests, electrodes with different spine diameters were investigated as well as tubes with diameters from 6.5 to 10.0 mm.

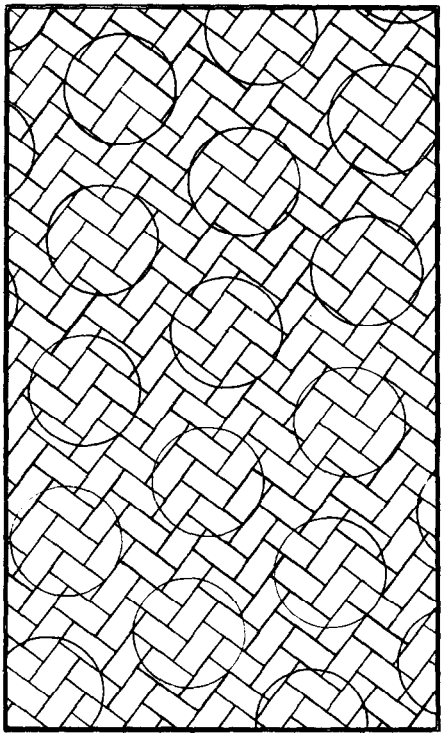

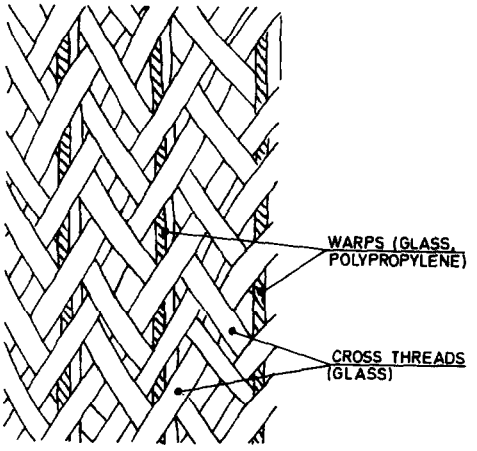

Fig. 1. The physical construction of the braided MP-tube (×15). The dark area is the perforated PVC wrapping.

Fig. 2. The physical construction of the braided HP-tube.

The permeability and electrical resistance of empty tubes were investigated in a simple apparatus constructed in the laboratory.

The construction of the cell unit is shown in Fig. 3. Almost all the experimental series consisted of 100 single cells, arranged in 10 groups, each of 10 replicate cells. The cell container was made of Plexiglass and the dimensions A and B (Fig. 3) were dependent on the diameter of the tubular electrode. The Porvic-type separator had a thickness of 2.0 mm. The two counter electrodes were ordinary negatives, 4.5 mm thick, and plane-parallel to two opposite walls. The spines had no star protrusions. Instead the centering of the spine was achieved by means of a cylindrical core during the filling procedure.

The alloy for the spines and the grids was lead–5.5 wt.% antimony.

The tubes were filled with a mixed powder containing 75 wt.% grey oxide (about 75 wt.% PbO and 25 wt.% Pb_{met}) and 25 wt.% red lead. The intensity and time of vibration were of decisive importance in reaching the required fill density. The weighed electrodes were then dipped into sulphuric acid of density 1.40 g/cm^3 for one hour. The surface was then rinsed for a few seconds with distilled water after which the electrodes were placed directly into the cell unit for formation. Formation acid 1.05 g/cm^3.

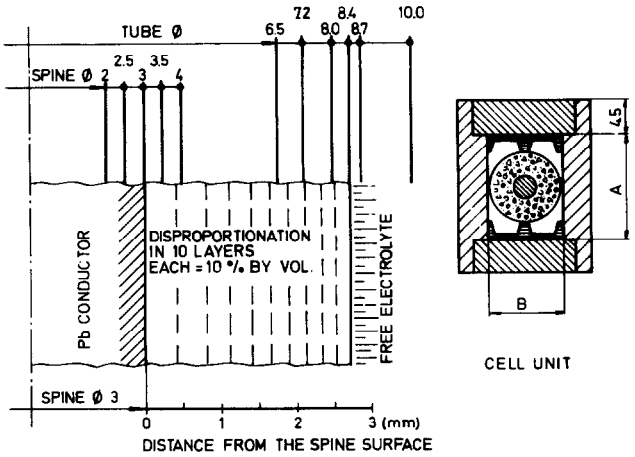

Fig. 3. The fundamentals of the work. Variables: 1, The material and construction of the tubes; 2, the diameter of the lead conductor; 3, the inner diameter of the tube; 4, the available volume of electrolyte; 5, the apparent density of the electroformed material. Constant conditions in electroforming, conditioning, and discharge routines, constant cell geometry in each series.

Formation programme

(1) 25 mA/cm^2 for 4 h (current density calculated on the geometrical area). Pause 2 h.

(2) 12.5 mA/cm^2 to a light gas evolution. Pause 2 h.

(3) 6.0 mA/cm^2 to normal gas evolution. Pause 2 h.

(4) 12.5 mA/cm^2 to vigorous gas evolution.

When the lead sulphate content was less than 1 wt.% by analysis the formation was considered to be completed.

After a change of acid to 1.28 g/cm^3 the cells were conditioned according to the schedule: discharge three times at 5 h rate to 1.73 V/cell and charge at the same rate to 140% of the 5 h capacity.

Before each test the acid concentration and volume were adjusted to the correct values. Each series of cells was discharged and charged under thermostatically controlled conditions at 25 °C.

The discharge routine was completed with a stepwise discharging process in order to achieve the current distribution profiles inside the electrodes.

Electrode soaking was performed in running distilled water for 24 h. Because of the protective wrapping and the running water the difficulties observed by Simonsson [21] were considered to have a negligible influence on the reaction products.

The washed and dried electrode was cut into three 45 mm pieces in a high speed lathe. Thirty millimetres of the wrapping was removed very carefully with a scalpel. The end with the 15 mm wrapping was carefully attached to a specially made, slightly soft holding device, *i.e.*, a self-centering chuck. The opposite rotating blades were constructed as cylinders with con-

cave-dished jaws. During the cutting procedure the cylinder was fed against the electrode. The stripped electrode then gradually moved into the cutting cylinder. The scaled material was collected in a transparent, covered container surrounding the cutting device.

The material was transferred with a soft brush into small pots and weighed. Another cutting cylinder of smaller diameter was attached and the procedure was repeated.

Generally, it was not difficult to cut 8 - 9 layers from the electrode, but when, sometimes, only 5 - 6 layers could be cut, a new electrode from the same batch was stripped.

Equivalent layers from the three pieces were collected in the pots, weighed, well mixed, and analyzed for sulphate ion, sometimes also for PbO and $PbO_{2-\delta}$, which, however, is not described in this report.

In excess of 2000 samples were analyzed.

The method does not include the reaction products of the three 15 mm wrapped pieces. It has, however, been shown in several investigations at our laboratory that the current distribution in short tubular electrodes is quite uniform vertically, with the exception of the upper tip where the initial current is a little higher than at the lower end. An equalization occurs after about the first 5% of the discharge time.

The chemical determination of the lead sulphate content of the discharged electrodes is a rather circumstantial procedure. In the literature one can find complexometric determinations with EDTA [23], but unfortunately the proposed indicators give a very indistinct colour change. The photometric determination of the end point, however, gives accurate results [24, 25] when the nonmetallic indicator (in this case thorin) is transferred to its metallic form. When the sample containing $PbSO_4$, PbO_2 and PbO is treated with a hot 10 wt.% ammonium acetate solution, $PbSO_4$ and PbO dissolve completely, while PbO_2 remains unattacked. The lead ions and other positive ions in the acetate solution are thereafter removed in an acidic cation exchanger (Amberlite IR 120). A measured volume diluted five times with acetone is then titrated with 0.01M $Ba(ClO_4)_2$ at pH 2.5.

The changes in absorbance are measured with a spot galvanometer and the point of inflection is obtained from a plot of the absorbance against the titration solution consumed. Percentage error max. ± 1.5.

The investigation of the impedance of single electrodes was carried out with a pulse generator in series with a potentiostat. A pulsating, square wave direct current (at a frequency of 1 Hz) was obtained. This current could be varied from 0 to 1000 mA. The electrode potential (here against a $Cd/CdSO_4$, $KHSO_4$ reference electrode with a Luggin capillary) was measured at 100, 200, 400, 800 and 1000 mA. A storage oscilloscope reproduced the transients. The arithmetic average of the straight-line (nearly vertical) parts, converted to ohms (or mΩ) according to Ohm's law, was used as a value of the electrode resistance. The capacitative part (the capacitance) of the impedance changes with the apparent density of the active material. It is, however, considered that two different electrodes with equal apparent density have

the same capacitance. A difference in a measured impedance could therefore be considered as a difference in ohmic resistance. The same equipment could also be used for the polarization tests.

Results and discussion

The double wall tube may be called a tube of *Medium Permeability* (MP), and the single wall tube a tube of *High Permeability* (HP).

(i) Some physical properties

The pressure drop with 10 l of air/min through the wall was 90 mm w.p. for MP-tubes and only 9 mm w.p. for HP-tubes.

The electrical resistance after 24 h in sulphuric acid was 0.35 Ω cm^{-2} for MP-tubes and 0.15 Ω cm^{-2} for HP-tubes.

(ii) Electrochemical properties

An examination of the most important electrochemical properties of porous electrodes is always a troublesome task. It was made, however, with a great number of single electrodes while carefully observing the operating conditions.

The electrode resistance (the impedance) including wrapping, lead conductor, and the acid in the pore system for MP and HP tubes with different amounts of active material (different apparent densities, AD) is shown in Fig. 4. It is evident that a high apparent density is favourable for the bulk resistance of the electrodes. The very small difference in resistance between electrode HP at 0 °C and electrode MP at +40 °C is remarkable.

The specific resistance in mΩ/g positive active material of a number of electrodes with tubes produced during different periods of research and development and tubes received from other manufacturers gives an impressive picture of the influence of the wall structure and the temperature of the electrolyte on the specific resistance of the electrodes (Fig. 5).

When measuring the overpotential the only way to obtain specific values for different electrodes is to treat completely electroformed electrodes, because then the only electrochemical reaction is the formation of oxygen.

The overpotential for HP and MP electrodes is shown in Fig. 6. Corrections for the resistive part are made from the straight-line part of the oscilloscope trace, as described earlier. The overpotential was measured from the starting-point of the curvature to a point 0.5 s later (see also Fig. 7). The values of overpotential are of particular interest for the charge acceptance at low temperatures. The observable higher overpotential of the MP electrode is the result of a non-uniform current distribution caused by the shielding effect of the outer wrapping, which rapidly causes a high current density in the PVC openings. These divergencies in electrochemical properties may therefore be a good indication of the specific suitability of the different

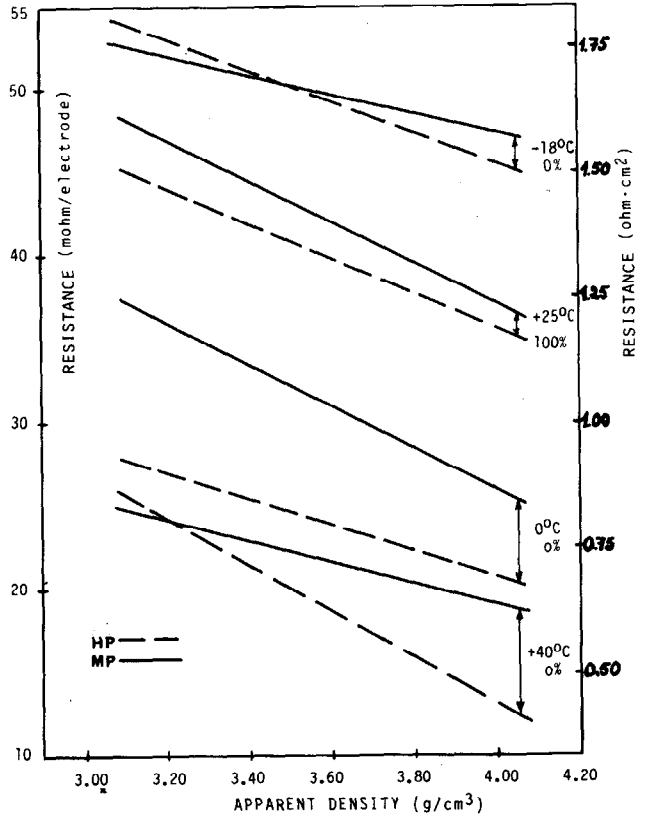

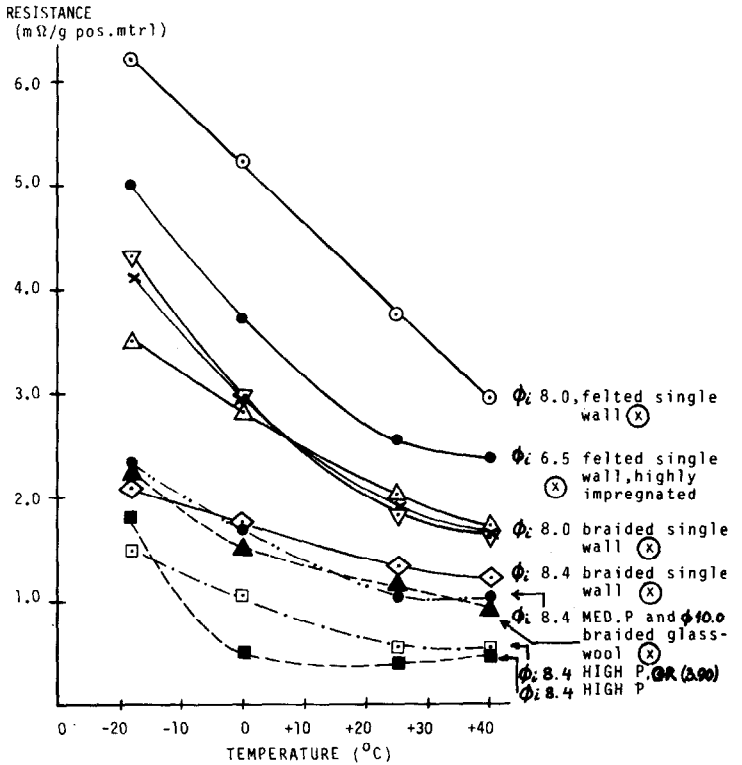

Fig. 4. The electrode resistance of HP and MP electrodes at different temperatures of the cell unit as a function of the apparent density. The construction of the two kinds of electrodes was identical regarding effective volume and geometry.

Fig. 5. The specific resistance of different tubular electrodes as a function of the temperature, the electrodes completely charged before measuring. Acid density 1.23 g/cm^3. Apparent density 3.65 g/cm^3, except for the high P tube with granulated oxide (GR). ϕ_i is the inner diameter of the tubes. ⊗ Means another manufacturer.

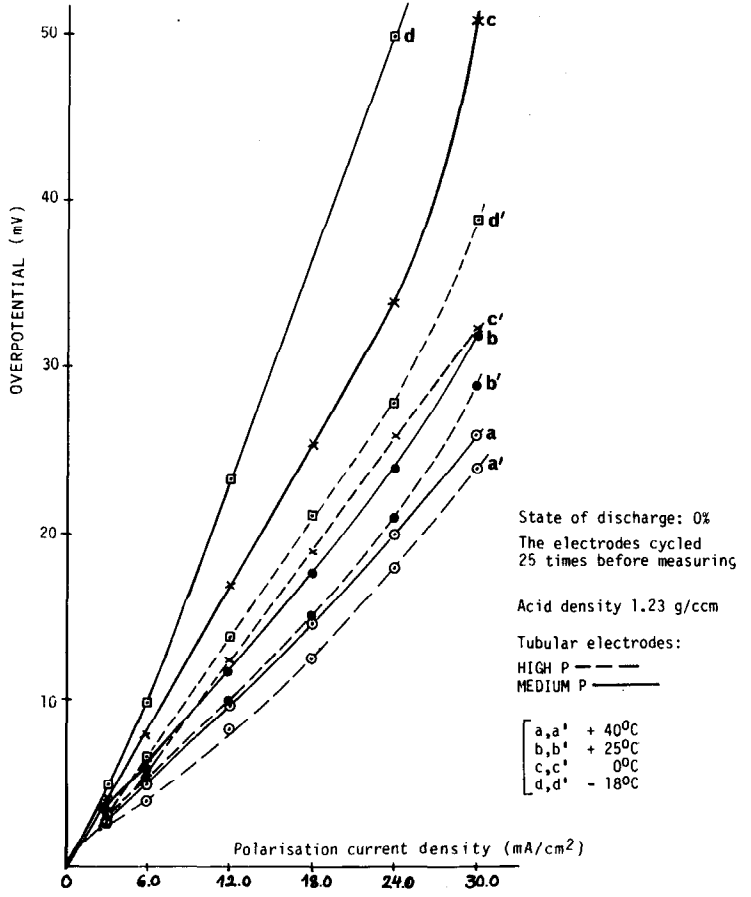

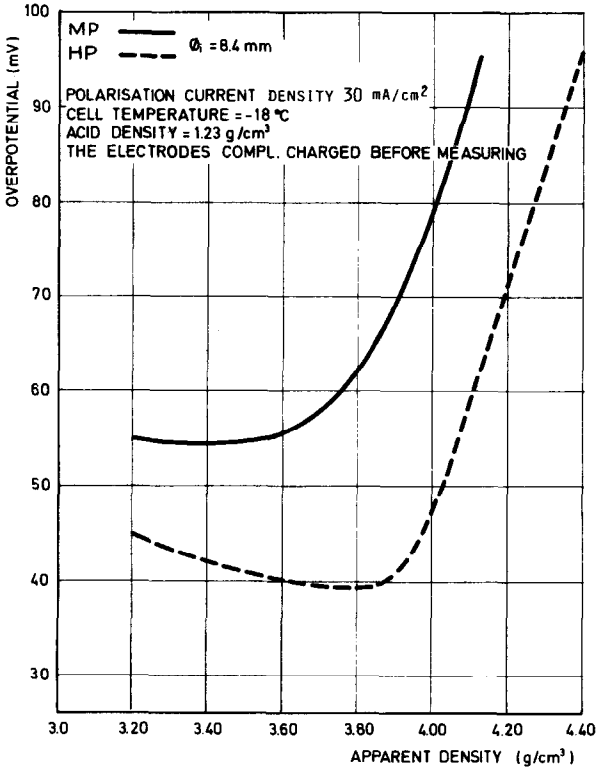

Fig. 6. The potential/current diagram for HP and MP electrodes. Apparent density 3.90 g/cm^3.

Fig. 7. The overpotential of HP and MP electrodes at −18 °C as a function of the apparent density of the active material. Polarisation current density, 30 mA/cm^2; cell temperature, −18 °C; acid density, 1.23 g/cm^3; the electrodes completely charged before measuring.

types of tubes for a variety of well-defined practical applications in the lead–acid cell. The reversible reactions which occur on discharge must consequently yield a higher output when using tubes with low resistance and overpotential.

It was finally of interest to study the dependence of overpotential in relation to the apparent density in the low temperature region (Fig. 7). With constant current density (30 mA/cm^2) there should be a decreasing current density when the apparent density increases, and consequently a decreasing overpotential. This happens for HP electrodes up to a certain apparent density (about 3.80 g/cm^3). The same tendency can be seen in the MP electrodes but over a much smaller range.

The most important observations are:

the sudden change to high overpotential for both types of electrodes;

the differences in mV between the curves.

Due to a direct oxygen evolution during measurement, the gas can pass more easily through the pore system at low apparent densities and can escape very easily through the wall of HP tubes.

Increasing apparent density also causes a constricted pore size and, in spite of decreasing current density, the adsorption and the clogging effect of oxygen bubbles will result in an extraordinary rise in overpotential. Accordingly, the wall structure of the tubes can be considered as an important factor in the design of tubular batteries.

(iii) The current distribution

The current distribution in the different layers investigated is presented in Figs. 9 - 14. The diagrams show the partial currents in each layer, calculated from the lead sulphate content. The sum of the currents through the material is the total discharge current or 100%.

These results were obtained with electrodes discharged to 25, 50, 75 and 100%, under the same conditions as described in the Experimental section. The lead sulphate content (g) of each layer was determined and their sum was compared with the amounts of lead sulphate calculated from Faraday's law. The coincidence is shown in Fig. 8. The discrepancies probably arise from the method of cutting the electrodes into three pieces and omitting 3×15 mm from the analysis. In Fig. 8, however, these are added to the other analyzed pieces with the assumption that they are of the same composition as the main pieces.

The change of porosity in the active material during a discharge period was observed with a mercury porosimeter. The porosity variations are of interest when calculating the optimum electrolyte content within and around electrodes of batteries with high performance qualities. Consequently, the dynamic relation, *i.e.*, the amount of acid directly available for an electrochemical reaction with the active material within the tube, is highly important.

If diffusion from the space around the electrode does not occur there will be a very rapid acid depletion in the pore system.

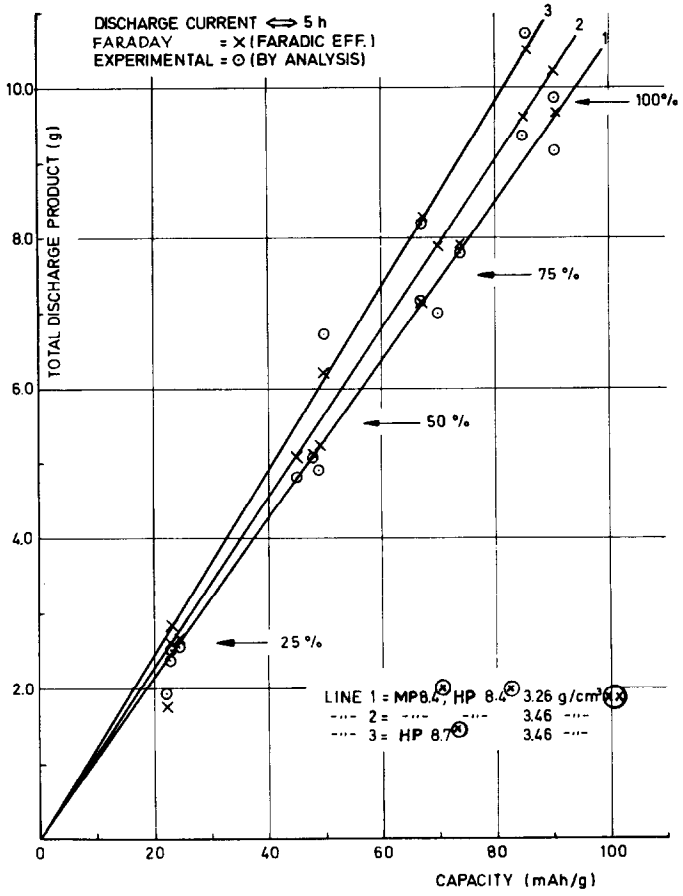

Fig. 8. Comparative values of Faraday and experimental amounts of discharge products. ⊗, inner diameter of the tubes; ⊗, apparent density.

The real need for acid during discharge can easily be calculated from the results of the analysis of the ten layers. The higher utilization of some layers and the competitive acid consumption for the negatives, however, makes dynamic control very difficult. With a distinct cell geometry based on a calculated dynamic relation and an estimated diffusion process, however, it was possible to obtain cell capacities higher than from a normal standard cell construction.

It is very clear that mass transport through the tube wall and within the pore system, the effective current paths, and the clogging effect of the reaction products greatly affect the current distribution throughout the active material. The tubes containing different amounts of active material have, in general, quite distinctive distribution curves at 25% as well as at 50% discharge time.

An interpretation of the first selection (Fig. 9) of the differential distribution curves, *i.e.* the percentage of total current, of electrodes chosen at

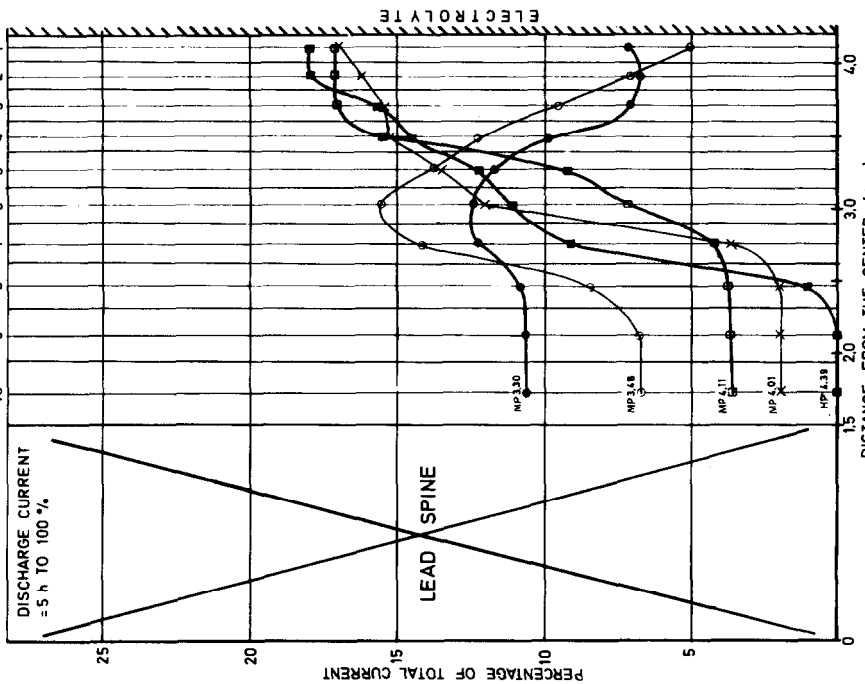

Fig. 9. Current distribution valid for MP and HP tubes. Apparent density 3.30 - 4.39 g/cm^3. State of discharge ~ 50%, spine diameter 3.0 mm.

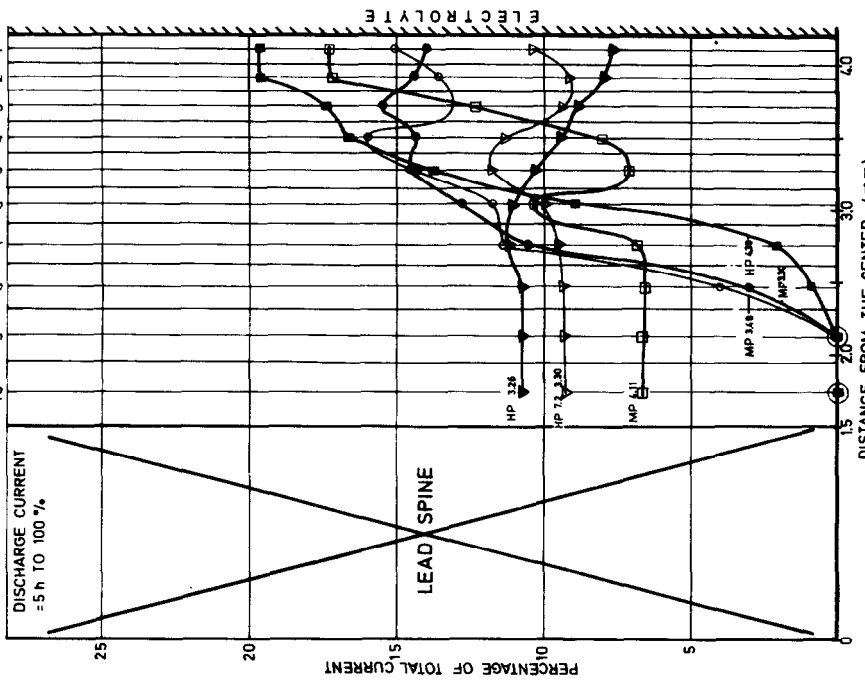

Fig. 10. Current distribution valid for MP and HP tubes. Apparent density 3.30 - 4.39 g/cm^3, state of discharge ~ 25%, spine diameter 3.0 mm.

random from cycled and 50% discharged cells at the 5 h current rate (about 18 mA/g) gives the following results:

— HP electrodes with low AD show a fairly uniform distribution. The effective factors are the open wall structure of the tube, the higher porosity of the active material and a sufficient amount of acid in the pore system.

— For MP electrodes with low AD the 4 - 6 outermost layers produce nearly the total Faraday current because of the shielding effect of the PVC, which causes a non-uniform distribution and a higher overpotential.

—HP and MP electrodes with high AD produce about the same profiles because of a lower ionic and a higher electronic conductivity of the compact active material.

Figure 10 shows the first 25% of the discharge time for the same series. The only difference is that the MP electrodes with low AD now also produce a more uniform profile throughout the layers. This is distinctive of all electrodes with low AD and, in general, is independent of the wall structure.

A direct comparison between MP and HP electrodes of the same size and with high apparent density is shown in Figs. 11 and 12. The stepwise discharge from zero to 100% at intervals of 25% reveals that the current distribution for MP electrodes (Fig. 11) is well pronounced. The very high utilization in the outer half volume of the active material during each period down to potential drop for MP electrodes is due to a constricted diffusion process.

The high efficiency for HP electrodes (Fig. 12) under the same conditions in an intermediate section, 75 - 100% of the discharge, is apparently caused by the open wall structure together with a favourable diffusion process in the pore system.

A survey of current profiles (Figs. 13 and 14) for HP electrodes with variations in the thickness of the active material, *i.e.*, tubular electrodes with tubes of different i.d., and for *Low*, *Medium*, *High* and *Very High* apparent densities would serve a useful purpose when searching for electrodes suitable for a well defined, practical application.

For tubes of equal i.d., Fig. 13(a) and (b), the total output capacity depends on the values of AD and the wall geometry. The differences in current profiles are especially noticeable for 25% and 100% discharge time.

The extremes of tube diameters, Fig. 14(a) and (b), *i.e.*, ϕ_i = 6.5 and 10.0 mm, can also show very good utilization of the active material if the apparent density is suitable; in this case *Low* AD for a thin layer and *Medium* AD for an extremely thick layer. Note the similarity of the curves in Figs. 13(a) and 14(b).

The amount of active material within the different types of tubes has, of course, a decisive influence on the capacity and, hence, determines the application of the lead–acid cell.

It was of interest to compare the differences in the integral capacity to 100% of HP and MP electrodes from five treated groups, *i.e.*, the average capacity of 10 layers from each of 25 electrodes (Fig. 15). With the values of MP as reference, the capacity curve for HP shows a pronounced maximum

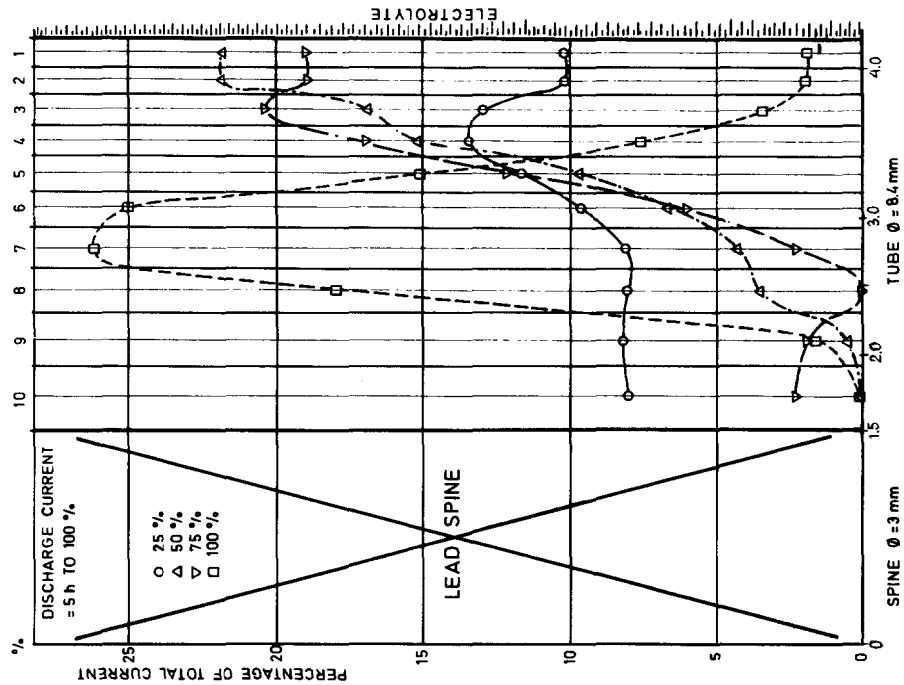

Fig. 11. Current distribution valid for MP 8.4 mm tube, apparent density 4.06 g/cm^3.

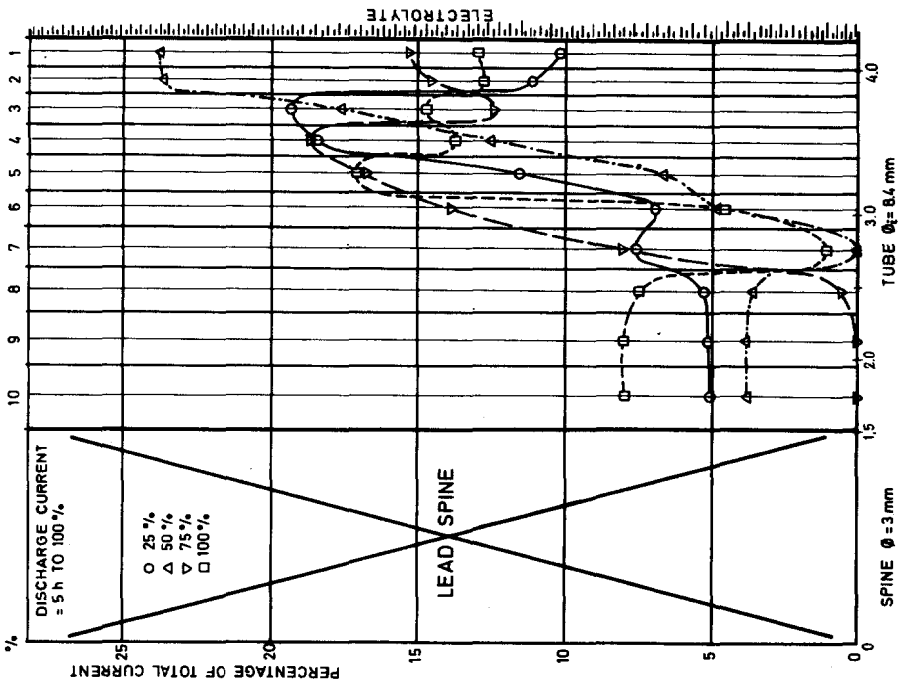

Fig. 12. Current distribution valid for HP 8.4 mm tube, apparent density 4.06 g/cm^3.

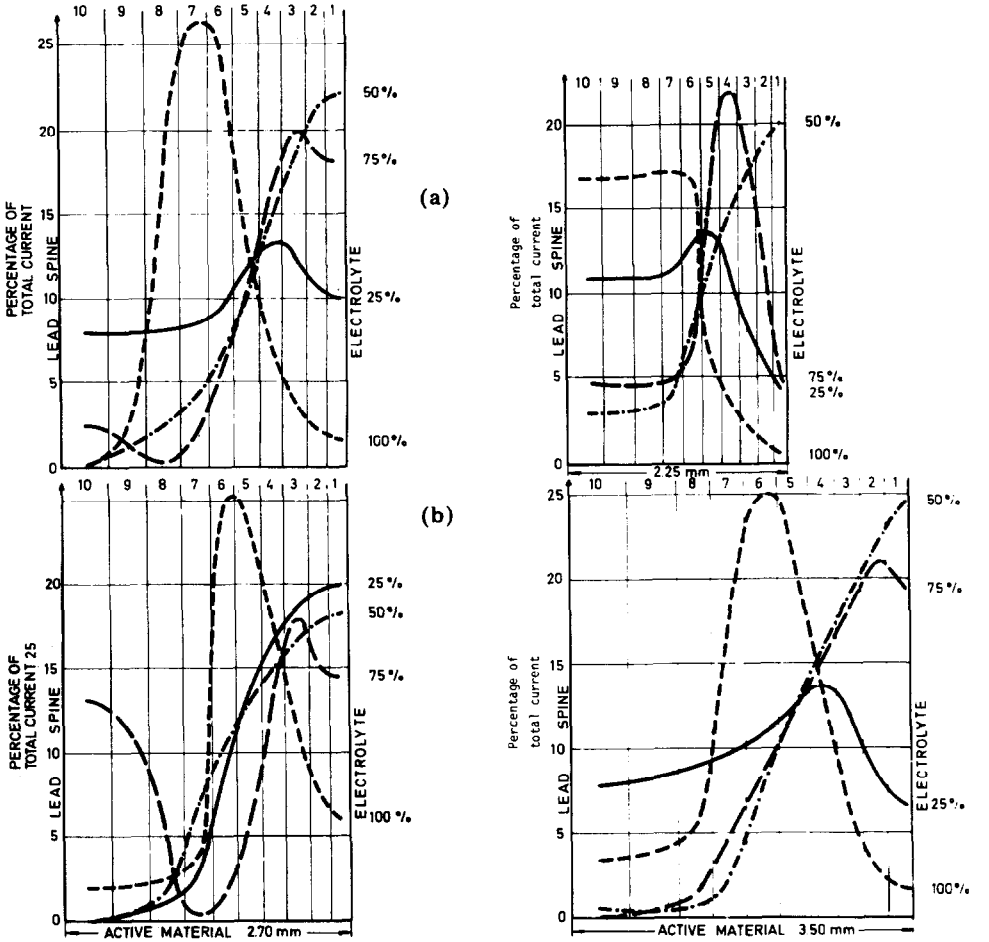

Fig. 13. Distribution profiles for electrodes with different apparent densities and inner diameters for the tube. Spine diameter 3.0 mm. (a) ϕ_i = 8.4 mm; High AD; 100% = 27.5 A h/PL. (b) ϕ_i = 8.4 mm; Very high AD, 100% = 25.5 A h/PL.

Fig. 14. Distribution profiles for electrodes with different apparent densities and inner diameters for the tube. (a) ϕ_i = 6.5 mm; low AD; 100% = 17.5 A h/PL; spine dia., 2.0 mm. (b) ϕ_i = 10.0 mm; medium AD; 100% = 29.8 A h/PL; spine dia., 3.0 mm.

in the 7th layer, while the three outermost layers for MP have a higher efficiency for the reasons mentioned earlier (*cf.* Fig. 11).

Considering the profiles in general, it will be evident that the active material around the lead spine can be divided approximately into three operative sections: an outer, an intermediate, and an inner section. The differences in capacity between the two types of electrodes are significant.

The need for an improved output capacity was certainly one outstanding requirement when scrutinizing the discharge efficiency of the porous electrodes in different experimental series. A simple means of emphasising

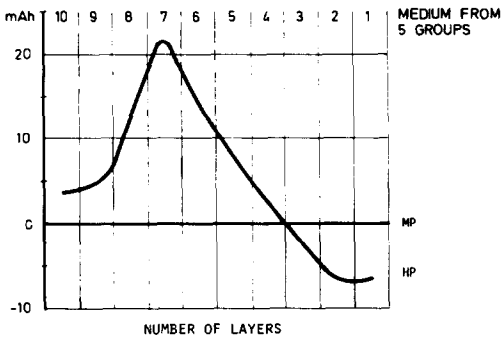

Fig. 15. Medium capacity difference for MP and HP electrodes.

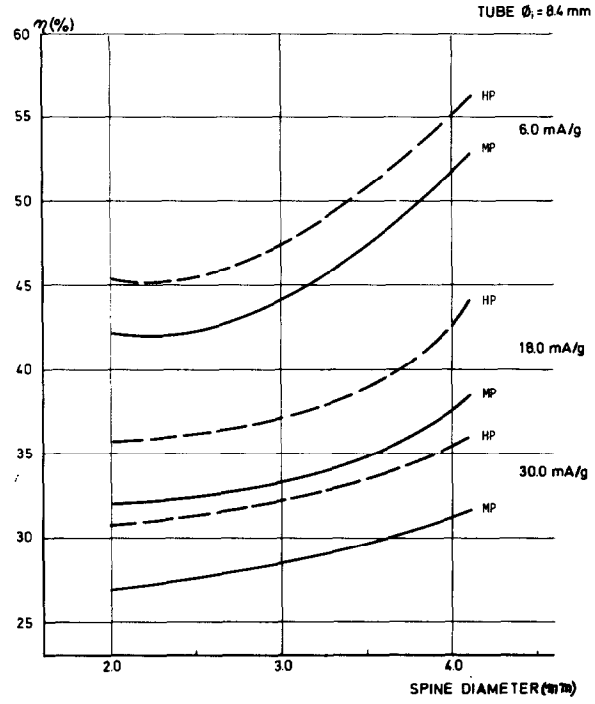

Fig. 16. The discharge efficiency as a function of the spine diameter. Apparent density 3.65 g/cm^3.

the importance of the thickness of the active material on the efficiency is illustrated in Fig. 16. The parameters are: the current density and the apparent density, the tube diameter, and HP *vs.* MP electrodes.

The most interesting result is the small difference between HP at 30 mA/g (= 1 h current) and MP electrodes at 18 mA/g (= 5 h current). Moreover, HP electrodes are always on a much higher level than the corresponding MP electrodes at all current densities.

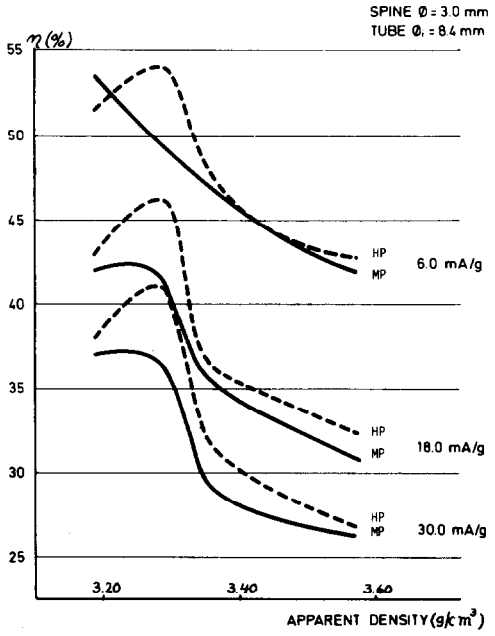

Fig. 17. The discharge efficiency as a function of the apparent density at different current densities.

As shown before, the apparent density of the electroformed material plays an important role in the proper utilization of the bulk material within the tubes. An interesting result within a rather narrow interval in apparent density can be seen in Fig. 17. It is of special importance for HP electrodes. The very steep drop accentuates the importance of a careful choice of the amount of lead oxide powder and its composition, the particle size distribution, the open pore volume, and the amount of free acid around the electrodes, *i.e.*, the cell geometry.

Therefore, the main effort in future work will be devoted to extensive studies of the structure of the active material and the geometrical construction of the positive electrodes and their effect on cycle life.

Acknowledgements

The author is grateful to Mr Ove Nilsson and Thore Eriksson for many constructive ideas and discussions concerning the experimental lay out. Mr Bo Rhodén is also thanked for the construction of the equipment for the electrochemical measurements, Mr. Sture Lindberg for the laborious machine work and Mr Holger Persson for the chemical analysis.

Finally, the author is indebted to Professor Olle Lindström for permission to complete this study in his department.

References

1 C. M. Shepherd, *J. Electrochem. Soc., 112* (1965) 252.
2 C. M. Shepherd, *J. Electrochem. Soc., 112* (1965) 657.
3 J. S. Newman and C. W. Tobias, *J. Electrochem. Soc., 109* (1962) 1183.
4 E. A. Grens II and C. W. Tobias, *Ber. Bunsenges. Phys. Chem., 68* (1964) 236.
5 J. Euler and W. Nonnenmacher, *Electrochim. Acta, 2* (1960) 268.
6 R. J. Brodd, *Electrochem. Technol., 6* (1968) 289.
7 J. J. Coleman, *J. Electrochem. Soc., 98* (1951) 26.
8 M. Bonnemay, G. Bronoel, E. Levart and A. A. Pilla, *J. Electroanal. Chem., 13* (1967) 58.
9 K. G. Soderberg, internal communication, AB Tudor, 1962.
10 A. Lindholm, internal communication, AB Tudor, 1965.
11 P. Ruetschi, J. Sklarchuk and R. T. Angstadt, *Electrochim. Acta, 8* (1963) 333.
12 W. Stein, *Dissertation*, Aachen, 1959.
13 J. Euler, *Electrochim. Acta, 7* (1962) 205.
14 J. Euler, *Electrochim. Acta, 15* (1970) 1233.
15 W. O. Butler, C. J. Venuto and D. V. Wiesler, *J. Electrochem. Soc., 117* (1970) 1339.
16 G. Sterr, *Electrochim. Acta, 15* (1970) 1221.
17 A. C. Simon, C. P. Wales and S. M. Caulder, *J. Electrochem. Soc., 117* (1970) 987.
18 J. Burbank, *J. Electrochem. Soc., 118* (1971) 525.
19 S. Tudor, A. Weisstuch and S. V. Davang, *Electrochem. Technol., 3* (1965) 90.
20 H. Haebler, H. Panesar and E. Voss, *Electrochim. Acta, 15* (1970) 1421.
21 D. Simonsson, *J. Electrochem. Soc., 120* (1973) 151.
22 E. Sundberg, *Second Int. Conf. on Lead, Aachen*, 1965.
23 G. Schwarzenbach, *Complexometric Titrations*, Methuen, London, 1957.
24 A. Ringbom, *Anal. Chim. Acta, 11* (1954) 153.
25 C. Wilson and D. Wilson, *Comprehensive Analytical Chemistry*, Vol IB, Elsevier, New York, 1960, pp. 318 - 320.